Radiology

Does the Functional Liver Imaging Score Derived from Gadoxetic Acid–enhanced MRI Predict Outcomes in Chronic Liver Disease?

Nina Bastati, MD • Lucian Beer, MD, PhD* • Mattias Mandorfer, MD, PhD • Sarah Poetter-Lang, MD • Dietmar Tamandl, MD • Yesim Bican, MD • Michael Christoph Elmer, BS, MD • Henrik Einspieler, MD • Georg Semmler, MD • Benedikt Simbrunner, MD • Michael Weber, PhD • Jacqueline C. Hodge, MD • Federica Vernuccio, MD, PhD • Claude Sirlin, MD, PhD • Thomas Reiberger, MD • Ahmed Ba-Ssalamah, MD*

From the Department of Biomedical Imaging and Image-Guided Therapy, Medical University of Vienna, General Hospital of Vienna (AKH), Waehringer Guertel 18-20, A-1090 Vienna, Austria (N.B., L.B., S.P.L., D.T., Y.B., M.C.E., H.E., M.W., J.C.H., A.B.); Hepatic Hemodynamic Laboratory, Medical University of Vienna, Vienna, Austria (M.M., G.S., B.S., T.R.); Division of Gastroenterology and Hepatology, Department of Internal Medicine III, Medical University of Vienna, Vienna, Austria (M.M., G.S., B.S., T.R.); Department of Health Promotion, Mother and Child Care, Internal Medicine and Medical Specialties, University of Palermo, Palermo, Italy (F.V.); and Liver Imaging Group, Department of Radiology, University of California, San Diego, La Jolla, Calif (C.S.). Received April 4, 2019; revision requested May 17; revision received August 13; accepted October 3. **Address correspondence to** A.B. (e-mail: *ahmed.ba-ssalamah@meduniwien.ac.at*).

*N.B. and L.B. contributed equally to this work.

Conflicts of interest are listed at the end of this article.

Radiology 2020; 294:98–107 • https://doi.org/10.1148/radiol.2019190734 • Content codes: GI MR

Background: Gadoxetic acid–enhanced MRI enables estimation of liver function in patients with chronic liver disease (CLD). The functional liver imaging score (FLIS), derived from gadoxetic acid–enhanced MRI, has been shown to predict transplant-free survival in liver transplant patients.

Purpose: To investigate the accuracy of the FLIS for predicting hepatic decompensation and transplant-free survival in patients with CLD.

Materials and Methods: Patients with CLD who had undergone gadoxetic acid–enhanced liver MRI, including T1-weighted volume-interpolated breath-hold examination sequences with fat suppression, performed between 2011 and 2015 were included. FLIS was assigned on the basis of the sum of three hepatobiliary phase features, each scored on an ordinal 0–2 scale: hepatic enhancement, biliary excretion, and the signal intensity in the portal vein. Patients were stratified into the following three groups according to fibrosis stage and a presence or history of hepatic decompensation: nonadvanced CLD, compensated advanced CLD (CACLD), and decompensated advanced CLD (DACLD). The predictive value of FLIS for first and/or further hepatic decompensation and for transplant-free survival was investigated by using Kaplan-Meier analysis, log-rank tests, and Cox regression analysis.

Results: This study evaluated 265 patients (53 years ± 14 [standard deviation]; 164 men). Intraobserver (κ = 0.98; 95% confidence interval: 0.97, 0.99) and interobserver (κ = 0.93; 95% confidence interval: 0.90, 0.95) agreement for FLIS were excellent. In patients with CACLD, the FLIS was independently predictive of a first hepatic decompensation (adjusted hazard ratio, 3.7; 95% confidence interval: 1.1, 12.6; $P = .04$), but not for further hepatic decompensations in patients with DACLD (adjusted hazard ratio, 1.4; 95% confidence interval: 0.9, 1.9; $P = .17$). The FLIS was an independent risk factor for mortality in both patients with CACLD (adjusted hazard ratio, 7.4; 95% confidence interval: 2.7, 20.2; $P < .001$) and those with DACLD (adjusted hazard ratio, 3.8; 95% confidence interval: 1.7, 9.5; $P = .004$).

Conclusion: The functional liver imaging score derived from gadoxetic acid–enhanced MRI identified patients with advanced chronic liver disease who are at increased risk for a first hepatic decompensation and for mortality.

Online supplemental material is available for this article.

Gadoxetic acid–enhanced MRI is used to depict and help characterize focal liver nodules (1,2) in patients with chronic liver diseases (CLDs) (3,4), including nonalcoholic steatohepatitis (5) and chronic hepatitis C (5,6). Gadoxetic acid–enhanced MRI has been shown to help predict both liver failure after subtotal hepatectomy and graft survival after liver transplant (7–9).

As laboratory and clinical estimators of liver disease severity, the albumin-bilirubin index, the Model for End-Stage Liver Disease, and the Child-Turcotte-Pugh score correlate well with gadoxetic acid uptake in the liver in the hepatobiliary phase (ie, 20 minutes after contrast agent administration of gadoxetic acid) (10,11). Previously described methods to assess hepatobiliary phase uptake include the relative liver enhancement, the hepatic uptake index, the contrast enhancement index, and T1 values (12). These methods all require complex computations and have vendor, field-strength, and sequence dependencies that complicate their clinical application.

Recently, Bastati et al (13) introduced the functional liver imaging score (FLIS), derived from the three hepatobiliary phase features of gadoxetic acid–enhanced MRI and each scored on an ordinal 0–2 scale. The three features included in the FLIS semiquantitatively assess the enhancement

Abbreviations

CACLD = compensated advanced CLD, CLD = chronic liver disease, DACLD = decompensated advanced CLD, FLIS = functional liver imaging score

Summary

The functional liver imaging score is a simple, noninvasive imaging marker that predicted transplant-free survival in patients with advanced, chronic liver disease.

Key Results

- An MRI-based functional liver imaging score (FLIS) is an independent risk factor for predicting mortality in patients with compensated and decompensated advanced chronic liver disease (adjusted hazard ratio, 7.44 [$P < .001$] vs 3.84 [$P = .004$], respectively).
- FLIS had an excellent interreader agreement with interclass correlation coefficients ranging between 0.89 and 0.98.
- FLIS may be used to predict an initial hepatic decompensation in patients with compensated advanced chronic liver disease (hazard ratio, 3.7; $P = .04$).

quality, the rate of biliary contrast excretion, and the persistence of signal intensity in the portal vein. Because the FLIS requires no signal intensity measurements, equations, or specific software, and is independent of MRI field-strength and vendor, it has the potential to be implemented easily in routine clinical practice. In a cohort of 128 patients who had undergone liver transplant (median follow-up, 36 months; range, 12–56 months) the FLIS was superior compared with clinical and laboratory parameters, including the Child-Turcotte-Pugh and Model for End-Stage Liver Disease, for the prediction of graft survival (13).

To our knowledge, no previous studies have evaluated the prognostic role of the FLIS in patients with CLD. The use of such an easy and reproducible score in clinical practice may potentially lead to better management of patients with CLD. We hypothesized that patients with a low FLIS are at higher risk for the development of hepatic decompensation and mortality compared with patients with a high FLIS.

The purpose of our study was to investigate the accuracy of the FLIS in predicting hepatic decompensation and transplant-free survival in patients with CLD.

Materials and Methods

Data regarding objective measurements (relative liver enhancement) that quantify the gadoxetic acid uptake in the hepatobiliary phase of this cohort were published previously (14). The research goals of our current study are different; our previous study assessed the inter- and intraobserver agreement of four different gadoxetic acid–enhanced MRI parameters and investigated their correlation with liver function parameters.

Patient Cohort

Our retrospective, single-center study was approved by the ethics committee of the Medical University of Vienna, and the study protocol conformed to the ethical guidelines of the 1975 Declaration of Helsinki.

The cohort was recruited in a single academic center, the Medical University of Vienna, from consecutive patients in our liver MRI database. All patients provided written informed consent before undergoing gadoxetic acid–enhanced (Primovist/Eovist; Bayer, Berlin, Germany) MRI on a 3.0-T imager between January 2011 and December 2015 ($n = 2791$). Inclusion and exclusion criteria are in Appendix E1 (online).

Clinical Data

Patient medical records were reviewed by two authors (G.S. and B.S.) under the supervision of specialists (M.M., a specialist in internal medicine, and T.R., a specialist in gastroenterology and hepatology, with 7 and 13 years of experience, respectively). The investigators reviewing the clinical information were blinded to any imaging information. Demographic and clinical data are shown in Table 1.

Disease Severity Classification

On the basis of the Fibrosis-4 score (cutoff, 1.45) (15) and previous history or current history of hepatic decompensation, patients were classified as having nonadvanced CLD (Fibrosis-4 score, ≤ 1.45), compensated advanced CLD (CACLD; Fibrosis-4 score, > 1.45), or decompensated advanced CLD (DACLD; history of or current hepatic decompensation). By using the following formula, we calculated the Fibrosis-4 score: age (years) $\times$ AST (U/L)/[PLT (10^9/L) $\times$ ALT$^{1/2}$(U/L)] (16), where *AST* is aspartate transaminase and *PLT* is platelet count.

Hepatic Decompensation and Transplant-Free Survival

Event-free survival time was defined from the time of MRI to the development of hepatic decompensation. We applied a commonly used definition of hepatic decompensation, including previous paracentesis, grade 3 or 4 hepatic encephalopathy, variceal bleeding, spontaneous bacterial peritonitis, and liver-related death (17–20). The details of the recurrent event analysis are in Appendix E1 (online). Transplant-free survival time was defined as the time from MRI to death or end of follow-up. For all analyses, patients who underwent liver transplant were censored on the day of operation.

MRI Protocol

Images from 3.0-T MRI (Magnetom Trio, A Tim; Siemens Healthcare, Erlangen, Germany) ($n = 265$) were obtained by using a combined six-element phased-array abdominal coil and a fixed spine coil. A standard dose of gadoxetic acid (0.025 mmol/kg; Primovist/Eovist, Bayer) was injected intravenously at a rate of 1.0 mL/sec and immediately followed by a 20-mL saline flush. The contrast-enhanced sequence consisted of three-dimensional T1-weighted volume-interpolated breath-hold examination sequences performed before and 20 minutes after contrast agent injection (section thickness, 1.7 mm; TR msec/TE msec, 2.67/0.92; field of view, 430 mm; flip angle, 13°). We performed axial in- and opposed-phase T1-weighted imaging (in-phase image parameters: section thickness, 5 mm; 130/2.46; field of view, 350 mm; and flip angle, 70°; opposed-phase image parameters: section thickness, 5 mm; 131/3.69; field of view, 350 mm; and flip angle, 70°), diffusion-weighted imaging (*b* values, 50, 300, and 600 sec/mm^2; section thickness, 6 mm; 1700/73; and field of view, 380 mm), and conventional T2-weighted imaging (sec-

Table 1: Comparison of Patient Characteristics between Patients with Nonadvanced Chronic Liver Disease, Compensated Advanced Chronic Liver Disease, and Decompensated Advanced Chronic Liver Disease

	Nonadvanced CLD (n = 56)			CACLD (n = 110)			DACLD (n = 99)		
Patient Characteristic	FLIS: 4–6 Points (n = 42)	FLIS: 0–3 Points (n = 14)	P Value	FLIS: 4–6 Points (n = 94)	FLIS: 0–3 Points (n = 16)	P Value	FLIS: 4–6 Points (n = 53)	FLIS: 0–3 Points (n = 46)	P Value
RLE	127.9 (88.7–163.3)	37.5 (26.2–46.1)	<.001	102.8 (74.8–126.1)	48.4 (29.4–58.7)	<.001	75.9 (52.4–92.9)	37.6 (25.6–53.5)	<.001
Mean age (y)	43 ± 12	42 ± 17	.95	56 ± 12	56 ± 18	.98	57 ± 11	54 ± 15	.23
Sex*									
Men	23 (55)	4 (29)	.13	57 (61)	8 (50)	.43	38 (72)	34 (74)	.83
Women	19 (45)	10 (71)		37 (39)	8 (50)		15 (28)	12 (26)	
Etiologic cause*			.003			.046			.41
HCV	5 (12)	1 (7)		29 (31)	0 (0)		11 (21)	5 (11)	
ALD	1 (2)	2 (14)		10 (11)	2 (13)		20 (38)	16 (35)	
HBV	5 (12)	0 (0)		9 (10)	0 (0)		6 (11)	2 (4)	
PSC	8 (19)	2 (14)		7 (7)	0 (0)		0 (0)	3 (6)	
Other	23 (55)	9 (65)		39 (41)	14 (87)		16 (30)	20 (44)	
HCC (development during follow-up)*	0 (0)	0 (0)	NA	5 (7)	0 (0)	.11	1 (4)	4 (5)	.85
CTP stage*									
A	NA	NA	NA	83 (88)	10 (63)	.02	10 (19)	0 (0)	.01
B	NA	NA	NA	11 (12)	6 (37)		35 (66)	28 (61)	
C	NA	NA	NA	0 (0)	0 (0)		8 (15)	18 (39)	
MELD, points	NA	NA	NA	9 (6–9)	13 (7–18)	<.001	13 (10–16)	19 (13–27)	<.001
Platelet count (G × L^{-1})	283 (203–336)	363 (234–514)	.03	135 (89–174)	158 (116–212)	.15	130 (80–158)	144 (82–180)	.43
Albumin (g × L^{-1})	42.9 (40.6–45.9)	37.0 (35.1–42)	<.001	39.8 (36.4–43.4)	33.6 (29.4–8.6)	<.001	34.2 (30.9–39.2)	30.4 (25.6–35.7)	.008
Bilirubin (mg × dL^{-1})	0.8 (0.3–0.9)	0.8 (0.4–0.9)	.64	1.0 (0.5–1.2)	4.0 (1.3–4.9)	<.001	2.0 (0.8–2.7)	6.4 (1.1–9.9)	<.001
INR	1.2 (1.1–1.2)	1.3 (1.1–1.3)	.57	1.3 (1.1–1.3)	1.4 (1.2–1.6)	.23	1.3 (1.1–1.4)	1.5 (1.2–1.6)	.003
Creatinine (mg × dL^{-1})	0.9 (0.7–1.0)	1.0 (0.7–1.1)	.18	0.9 (0.7–1.0)	0.9 (0.6–1.1)	.71	1.1 (0.7–1.2)	1.6 (0.7–2.3)	.04
Sodium (mmol × L^{-1})	139 (137–142)	138 (136–140)	.15	140 (138–142)	138 (134–141)	.20	137 (133–141)	134 (132–137)	.006
ALP (U × L^{-1})	121 (68–132)	171 (57–214)	.12	106 (67–125)	138 (88–219)	<.001	126 (85–143)	166 (79–212)	.06
GGT (U × L^{-1})	123 (22–221)	198 (52–317)	.33	160 (41–170)	160 (50–281)	.30	141 (54–153)	156 (49–235)	.50
AST (U × L^{-1})	35 (23–42)	38 (22–44)	.67	55 (29–63)	72 (34–127)	.01	47 (28–56)	57 (34–108)	.04
ALT (U × L^{-1})	29 (20–54)	32 (19–54)	.85	34 (21–57)	42 (17–85)	.02	26 (18–41)	35 (22–59)	.05
Hepatic fat percentage	4.4 (0–11.4)	3.7 (0.6–12.6)	.59	5.9 (2.5–10.1)	4.1 (0.4–6.3)	.22	4.1 (0.1–7.4)	1.5 (0–6.1)	.94

Note.—Unless otherwise indicated, data in parentheses are interquartile range; mean data are ± standard deviation. ALD = alcoholic liver disease, ALP = alkaline phosphatase, ALT = alanine transaminase, AST = aspartate transaminase, CACLD = compensated advanced CLD, CLD = chronic liver disease, CTP = Child-Turcotte-Pugh, DACLD = decompensated advanced CLD, FLIS = functional liver imaging score, GGT = γ-glutamyltransferase, HBV = hepatitis B, HCC = hepatocellular carcinoma, HCV = hepatitis C, INR = international normalized ratio, MELD = model for end-stage liver disease, NA = not applicable, PSC = primary sclerosing cholangitis, RLE = relative liver enhancement.

* Data are numbers and data in parentheses are percentages.

tion thickness, 5 mm; 1800/150; field of view, 400 mm; and flip angle, 150°), including coronal MRI cholangiopancreatography (section thickness, 45 mm; 5500/454; field of view, 380 mm; and flip angle, 180°) and T2-weighted half-Fourier rapid acquisition with relaxation enhancement sequences (section thickness, 4.5 mm; 805/76; field of view, 450 mm; and flip angle, 141°). MRI parameters are provided in Table E1 (online).

Image Analysis

Three radiologists (N.B., radiologist 1, board-certified with ≥8 years of experience in abdominal imaging; A.B., radiologist 2, with ≥20 years of experience in abdominal imaging; and L.B., radiologist 3, who is in the 4th year of training) independently analyzed axial unenhanced and axial and coronal hepatobiliary phase–enhanced MRI on a picture archiving and communication system (Impax; Agfa, Mortsel, Belgium). Radiologist 1 again analyzed 100 randomly selected examinations after a 4-week interval to assess intrareader repeatability. The radiologists were blinded to all clinical, histologic, and laboratory data. In addition, radiologist 1 read the coronal T2-weighted two- and three-dimensional images from MRI cholangiopancreatography and T2-weighted half-Fourier rapid acquisition with relaxation enhancement images, looking for bile duct dilatation, which was considered suspicious for mechanical obstruction. Consequently, those patients were excluded from further analysis (n = 13).

Before analyzing the images from the patient cohort, the radiologists jointly reviewed the MRI criteria by reviewing 50 gadoxetic acid–enhanced MRI examinations in patients who had undergone liver transplant and were not part of our cohort.

On the basis of axial and coronal hepatobiliary phase−enhanced MRI, we determined the following:

1. Enhancement quality score of 0, 1, or 2 compared the liver to right kidney uptake. A score of 0, 1, or 2 was assigned if the liver was hypo-, iso-, or hyperintense respectively, to the right kidney.

2. Excretion quality score of 0, 1, or 2 was determined on the basis of the degree of contrast agent excretion into the biliary tract. A score of 0, 1, or 2 was assigned if there was no biliary tract contrast beyond the common hepatic duct or contrast reached at least to the duodenum.

3. The portal vein sign quality score of 0, 1, or 2 was on the basis of the portal vein relative to liver parenchymal signal intensity. A score of 0, 1, or 2, respectively, was assigned if the portal vein was hyper-, iso-, or hypointense to the liver parenchyma (Table 2).

The FLIS, ranging from 0 to 6 points, represented the sum of the above three parameters because they all had an equal weighting on the transplant-free survival (13). See examples in Figure 1. We also calculated the relative liver enhancement and hepatic fat fraction, listed in Appendix E1 (online).

Statistical Analysis

Statistical analyses were performed by using commercially available statistical software (SPSS Statistics Version 24, IBM, Armonk, NY; and GraphPad Prism Version 5.01, GraphPad Software, La Jolla, Calif). Multievent analysis was performed with open-source software (R version 3.5.1; R Foundation for Statistical Computing, Vienna, Austria) by using the survival package (21,22).

Table 2: Definition and Grading System for the Three FLIS Parameters

Parameter	Points
Liver parenchymal enhancement quality score	
SI of liver parenchyma relative to kidney on HBP	
Hypointense	0
Isointense	1
Hyperintense	2
Biliary contrast excretion quality score	
Presence of contrast media in the bile ducts 20 min after contrast application	
No biliary contrast excretion	0
Excretion into peripheral intrahepatic bile ducts or the right and/or left hepatic duct(s)	1
Excretion into the common hepatic duct, the common bile duct, or the duodenum	2
Portal vein sign PVsQS	
SI of the portal vein relative to the liver parenchyma 20 min after contrast application	
Hyperintense	0
Isointense	1
Hypointense	2

Note.—SI = signal intensity, HBP = hepatobiliary phase, PVsQS = portal vein sign quality score.

Continuous variables were reported as mean and standard deviation for normally distributed data or, for skewed data, medians with interquartile ranges; categorical variables were reported as number and percentage of patients with specific characteristics.

One-way analysis of variance was used for group comparisons of continuous variables, when applicable. Otherwise, a Kruskal-Wallis test was applied. Group comparisons of categorical variables were performed by using the χ^2 or Fisher exact test, as appropriate.

Intraobserver and interobserver variability were obtained by using a mixed intraclass correlation coefficient model, with absolute agreements, single measures, and 95% confidence intervals.

Receiver operating characteristic curve analysis was performed to differentiate between patient groups and the optimal cut-off values were estimated according to the Youden index (23).

To identify independent predictors for repeated hepatic decompensations over the course of disease, we used the Prentice-Williams and Peterson model with a gap-time scale by using the survival package in R (R Foundation for Statistical Computing). The association between FLIS, clinical data, first hepatic decompensation, and transplant-free survival was investigated by using Kaplan-Meier analysis, log-rank tests, and Cox regression. For each group, the identified risk factors in the Kaplan-Meier analysis were further tested in the Cox regression analysis. A two-sided P value of .05 or less was considered to indicate statistical significance.

Results

Characteristics of Study Sample

Figure 2 shows the patient accrual flowchart. Our study sample included a well-characterized cohort of 265 patients

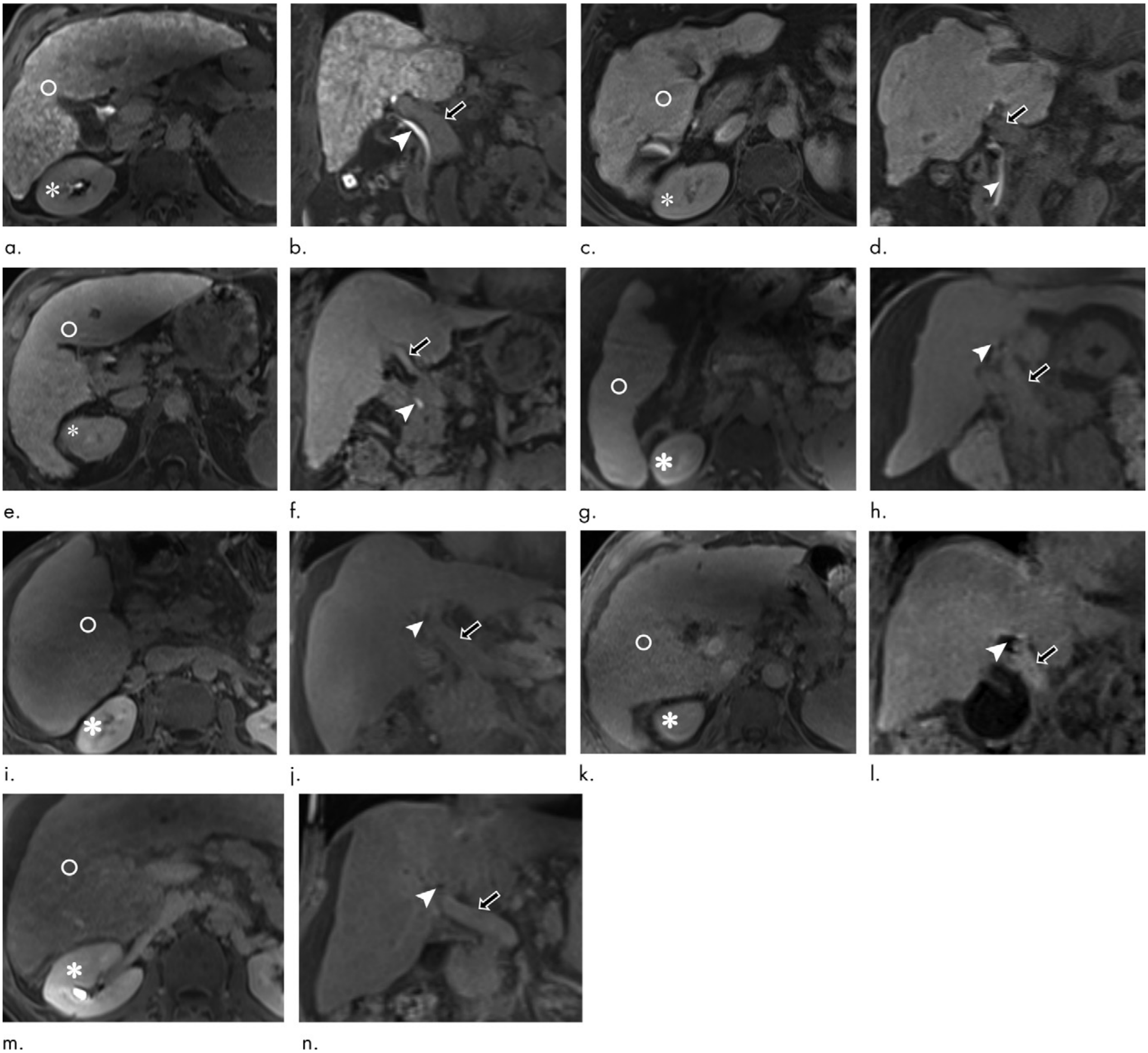

Figure 1: Images from 3.0-T MRI obtained 20 minutes after gadoxetic acid administration in the axial and coronal planes in seven patients with advanced chronic liver disease. **(a, b)** A 61-year-old man with alcohol-induced cirrhosis with functional liver imaging score (FLIS) of 6; liver parenchymal enhancement quality score is 2 because the signal intensity of the liver (circle) is higher than that of the right kidney (*). Excretion quality score is 2 because contrast media is in the common bile duct (arrowhead). Portal vein sign quality score is 2 because the portal vein (arrow) is hypointense to the liver parenchyma. **(c, d)** Images in a 65-year-old woman with primary biliary cirrhosis. FLIS of 5. Enhancement quality score is 1 because the liver signal intensity (circle) is similar to that of the right kidney (*). The excretion quality score is 2 because contrast media is in the common bile duct (arrowhead). Portal vein sign quality score is 2 because portal vein (arrow) is hypointense to the liver parenchyma. **(e, f)** Images in a 52-year-old man with alcohol-induced cirrhosis. FLIS of 4. Enhancement quality score is 1 because liver signal intensity (circle) is similar to that of the right kidney (*). Excretion quality score is 2 because contrast media is in the common bile duct (arrowhead). Portal vein sign quality score is 1 because portal vein (arrow) is isointense to the liver parenchyma. **(g, h)** Images in a 50-year-old man with alcoholic liver disease. FLIS of 3. Enhancement quality score is 1 because the liver signal intensity (circle) is similar to that of right kidney (*). Excretion quality score is 1 because contrast media is not seen distal to intrahepatic bile ducts (arrowhead). Portal vein sign quality score is 1 because the portal vein (arrow) is isointense to liver parenchyma. **(i, j)** Images in a 50-year-old man with alcoholic liver disease. FLIS of 2. Enhancement quality score is 0 because the liver signal intensity (circle) is lower than that of the right kidney (*). Excretion quality score is 1 because contrast media is not seen beyond the intrahepatic bile ducts (arrowhead). Portal vein sign quality score is 1 because the portal vein (arrow) is isointense to liver parenchyma. **(k, l)** Images in a 50-year-old man with cirrhosis from nonalcoholic steatohepatitis. FLIS of 1. Enhancement quality score is 1 because liver signal intensity (circle) is equal to that of the right kidney (*). Excretion quality score is 0 because no contrast media is seen in the biliary tree (arrowhead). Portal vein sign quality score is 0 because the portal vein (arrow) is hyperintense to the liver parenchyma. **(m, n)** Images in a 69-year-old man with hepatitis C virus cirrhosis. FLIS of 0. Enhancement quality score is 0 because the liver signal intensity (circle) is less than that of the right kidney (*). Excretion quality score is 0 because no contrast media is in the biliary tree (arrowhead). The portal vein sign quality score is 0 because portal vein signal intensity (arrow) is greater than that of the liver parenchyma.

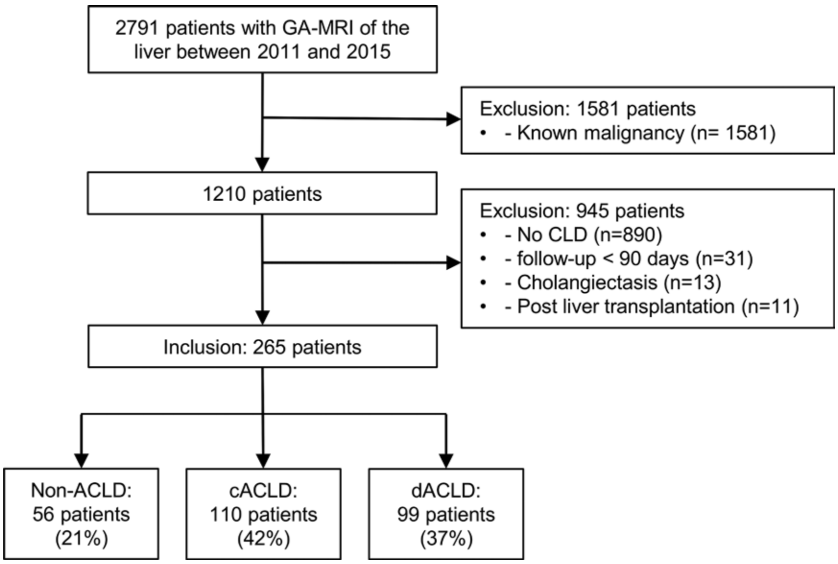

Figure 2: Study flowchart of included patients from the institutional database. Patients with gadoxetic acid (GA)-enhanced MRI, performed between 2011 and 2015, were included. After applying the exclusion criteria, 265 patients were categorized into three groups: nonadvanced chronic liver disease (non-ACLD), compensated advanced chronic liver disease (cACLD), and decompensated advanced chronic liver disease (dACLD). CLD = chronic liver disease.

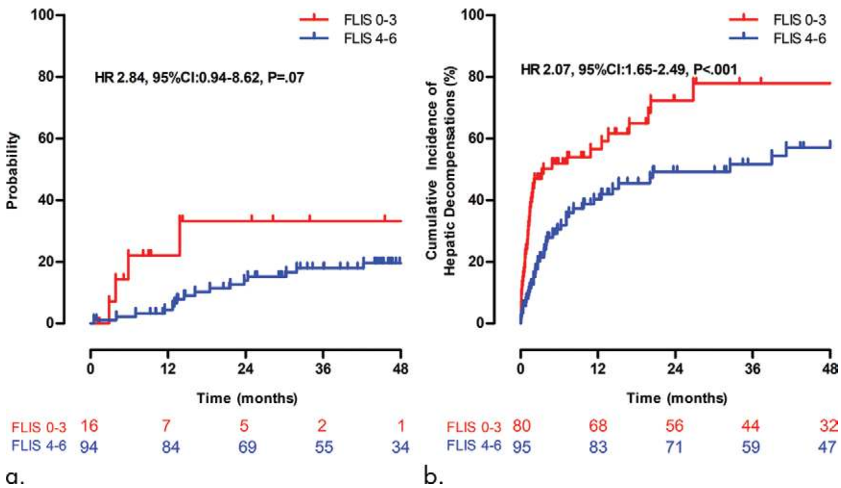

Figure 3: Kaplan-Meier curves for first and recurrent hepatic decompensation. **(a)** First hepatic decompensation in patients with compensated advanced chronic liver disease and **(b)** recurrent hepatic decompensation in patients with decompensated advanced chronic liver disease (DACLD). A multievent analysis was used to assess the development of recurrent hepatic decompensations in patients with DACLD. CI = confidence interval, FLIS = functional liver imaging score, HR = hazard ratio.

(164 men and 101 women) with CLD (mean age, 53 years ± 14 [standard deviation]). Patients with nonadvanced CLD, CACLD, and DACLD were followed up for a median of 40.7, 40.6, and 13.7 months, respectively. The most common causes of CLD were viral hepatitis (hepatitis C virus, 51 of 265 patients [19.2%]; and hepatitis B virus, 22 of 265 patients [8.3%]) and alcoholic liver disease (51 of 265 patients; 19.2%). On the basis of the Fibrosis-4 score (cutoff, 1.45) for the exclusion of advanced liver fibrosis and the presence or absence of previous or current hepatic decompensation, patients were classified as nonadvanced CLD (56 of 265 patients; 21.1%), CACLD (110 of 265 patients; 41.5%), or DACLD (99 of 265 patients; 37.4%) (Table 1).

Reader Agreement for the FLIS Score

Intraobserver intraclass correlation coefficient for FLIS for radiologist 1 was 0.98 (95% confidence interval: 0.97, 0.99). Interobserver intraclass correlation coefficients (κ) for FLIS were as follows: for radiologist 1 versus radiologist 2, 0.93 (95% confidence interval: 0.90, 0.96); for radiologist 1 versus radiologist 3, 0.89 (95% confidence interval: 0.86, 0.92); and for radiologist 2 versus radiologist 3, 0.92 (95% confidence interval: 0.88, 0.95). All intraclass correlation coefficients indicated excellent agreement. Subsequent results are provided only for the more experienced radiologist (ie, radiologist 2).

Quantitative Assessment of the Enhancement Score

We compared the liver-to-kidney signal intensity on hepatobiliary phase images to evaluate whether results from our semiquantitative assessment were reflected by actual differences in the signal intensity. In patients with enhancement quality scores of 0, the right kidney signal intensity was higher than that of the liver (355 ± 117 vs 301 ± 72, respectively; $P < .001$) and was lower in patients with enhancement quality scores of 2 (405 ± 106 vs 573 ± 120, respectively; $P < .001$) (Fig E1 [online]). In patients with enhancement quality scores of 1, there was no difference between the signal intensity of the kidney and liver (399 ± 132 vs 392 ± 96, respectively; $P = .62$).

FLIS Stratification

The optimal cutoff for the FLIS to predict 12 months of transplant-free survival was 4 points, which resulted in a sensitivity of 92% (87 of 95) and a specificity of 58% (seven of 12) in the CACLD group and a sensitivity of 71% (37 of 52) and a specificity of 81% (25 of 31) in the DACLD group. Patients were therefore stratified according to their FLIS, indicating impaired (FLIS, 0−3) or preserved (FLIS, 4−6) hepatic function. The clinical and laboratory data from the three patient groups, stratified according to FLIS points, are in Table 1.

Hepatic Decompensation

As expected, no patients in the nonadvanced CLD group developed hepatic decompensation. Twenty-one (19.1%) of 110 patients in the CACLD group developed hepatic decom-

Table 3: Influence of Demographic and Clinical Data on Decompensation in Compensated Advanced Chronic Liver Disease and Recurrent Hepatic Decompensation in Patients with Decompensated Advanced Chronic Liver Disease

	Univariable Analysis in CACLD (*n* = 110)		Multivariable Analysis in CACLD (*n* = 110)		Univariable Analysis in DACLD (*n* = 99)		Multivariable Analysis in DACLD (*n* = 99)	
Patient Characteristic	Hazard Ratio	*P* Value	Hazard Ratio	*P* Value	Hazard Ratio	*P* Value	Hazard Ratio	*P* Value
FLIS (0–3 vs 4–6 points)	2.8 (0.94, 8.62)	.07	3.7 (1.10, 12.64)	.04	2.1 (1.65, 2.49)	<.001	1.4 (0.9, 1.9)	.17
RLE	0.99 (0.98, 1.00)	.17			0.99 (0.98, 1.00)	.002	1.00 (0.99, 1.01)	.74
Hepatic fat percentage	0.97 (0.91, 1.04)	.37			1.00 (0.97, 1.04)	.79		
Age	1.0 (0.96, 1.03)	.82			1.02 (1.00, 1.04)	.02	1.02 (1.00, 1.04)	.02
Sex (men vs women)	1.01 (0.42, 2.40)	.98			1.4 (0.91, 1.93)	.24		
MELD (per point)	1.03 (0.94, 1.12)	.56			1.1 (1.05, 1.10)	<.001	1.06 (1.03, 1.09)	<.001
Platelet count (per G × L^{-1})	1.00 (0.98, 1.00)	.04	0.99 (0.98, 1.00)	.04	1.00 (0.99, 1.00)	.21		
Albumin (per g × L^{-1})	0.90 (0.84, 0.95)	.002	0.92 (0.85, 0.99)	.03	0.95 (0.93, 0.98)	.008	0.96 (0.92, 0.99)	.003
Bilirubin (per mg × dL^{-1})	1.04 (0.82, 1.30)	.77			1.06 (1.02, 1.09)	.005		
INR	1.1 (0.37, 3.23)	.89			1.6 (1.08, 2.07)	.11		
Creatinine (per mg × dL^{-1})	2.2 (0.91, 5.52)	.09			1.4 (1.22, 1.62)	.006		
Sodium (per mmol × L^{-1})	1.02 (0.91, 1.14)	.76			0.94 (0.91, 0.98)	.005		
ALP (per U × L^{-1})	1.00 (1.00, 1.00)	.71			1.00 (1.00, 1.00)	.67		
GGT (per U × L^{-1})	1.01 (1.00, 1.00)	.1			1.00 (1.00, 1.00)	.08		
AST (per U × L^{-1})	1.01 (1.00, 1.00)	.9			1.00 (1.00, 1.00)	.2		
ALT (per U × L^{-1})	0.99 (0.97, 1.00)	.12			1.00 (1.00, 1.00)	.39		

Note.—Data in parentheses are 95% confidence intervals. ALP = alkaline phosphatase, ALT = alanine transaminase, AST = aspartate transaminase, CACLD = compensated advanced chronic liver disease, DACLD = decompensated advanced chronic liver disease, FLIS = functional liver imaging score, GGT = γ-glutamyltransferase, INR = international normalized ratio, MELD = model for end-stage liver disease, RLE = relative liver enhancement.

pensation; of these 110 patients, eight (7.3%) had a second event and one (0.9%) had a third and fourth event. Sixty (61%) of 99 patients in the DACLD group had a decompensating event during the follow-up; of these 99 patients, 22 patients (22%) developed a second event and three (3%) developed a third and fourth event.

In the CACLD group, platelet count (P = .04), serum albumin levels (P = .03), and FLIS (adjusted hazard ratio, 3.7; 95% confidence interval: 1.1, 12.6; P = .04) (Fig 3a, Table 3) were identified as independent risk factors for the development of a first hepatic decompensation. Because these patients may also have repeated events, we analyzed the same CACLD cohort by using the multievent analysis, which showed that albumin, γ-glutamyltransferase, and alanine transaminase levels were associated with the development of recurrent hepatic decompensations (P = .03, $P < .001$, and P = .02, respectively), whereas the FLIS was not an independent risk factor (hazard ratio, 1.7; 95% confidence interval: 0.7, 2.6; P = .19) for the development of recurrent events in patients with CACLD (Fig E2, Table E2 [online]).

In the DACLD group, patient age, Model for End-Stage Liver Disease, and albumin levels were independent risk factors for recurrent hepatic decompensations (P = .02, $P <$ .001, and P = .003, respectively). Although the FLIS was identified as a risk factor for recurrent decompensation in the univariable analysis (hazard ratio, 2.1; 95% confidence interval: 1.7, 2.5; $P < .001$) (Fig 3b), it was not an independent predictor in the multivariable analysis (P = .17).

Transplant-Free Survival

Nine of 110 patients (8.2%) in the CACLD group underwent liver transplant and 24 patients (21.8%) died. Nineteen of 99 patients (19%) in the DACLD group underwent liver transplant and 48 patients (49%) died (Table 4).

In the CACLD group, albumin levels and the FLIS (adjusted hazard ratio, 7.4; 95% confidence interval: 2.7, 20.2; $P < .001$) (Fig 4a) were the only independent risk factors for lower transplant-free survival.

In the DACLD group, age, the Model for End-Stage Liver Disease score, albumin levels, and the FLIS (adjusted hazard ratio, 3.8; 95% confidence interval: 1.2, 9.5; P = .004) (Fig 4b) were independent risk factors for death.

Distribution of the FLIS in a Cohort of Patients without CLD

A cohort of 738 patients (mean age, 49 years ± 15; 427 women) without CLD was used to evaluate the distribution of the FLIS. All patients had a FLIS of 4 points or more (6 points, 693 of 738 patients [93.9%]; 5 points, 28 of 738 patients [3.8%]; and 4 points, 16 of 738 patients [2.2%]).

Discussion

The functional liver imaging score (FLIS) is a semiquantitative scoring system on the basis of three hepatobiliary phase−derived features obtained 20 minutes after injection of gadoxetic acid. It was shown previously that the FLIS can predict retransplant-free survival in patients after liver transplant (13). Our study demonstrates that the FLIS is an independent

Table 4: Influence of Demographic and Clinical Data on Transplant-Free Survival in Patients with Nonadvanced Chronic Liver Disease, Compensated Advanced Chronic Liver Disease, and Decompensated Advanced Chronic Liver Disease

	Univariable Analysis in Nonadvanced CLD (n = 56)		Univariable Analysis in CACLD (n = 110)		Multivariable Analysis in CACLD (n = 110)		Univariable Analysis in DACLD (n = 99)		Multivariable Analysis in DACLD (n = 99)	
Patient Characteristic	Hazard Ratio	P Value	Hazard Ratio	P Value	Hazard Ratio	P Value	Hazard Ratio	P Value	Hazard Ratio	P Value
FLIS (0–3 vs 4–6 points)	5.7 (0.94, 34.5)	.06	7.73 (3.0, 20.0)	<.001	7.44 (2.74, 20.17)	<.001	5.16 (2.6, 10.1)	<.001	3.84 (1.1, 9.5)	.004
RLE	0.96 (0.96, 1.00)	.05	0.99 (0.98, 1.00)	.06			0.98 (0.96, 0.99)	.001	1.01 (1.00, 1.03)	.15
Hepatic fat percentage	0.96 (0.82, 1.12)	.60	0.99 (0.93, 1.05)	.70			0.99 (0.94, 1.05)	.82		
Age (per year)	1.01 (0.94, 1.08)	.99	1.02 (0.98, 1.06)	.32			1.03 (1.01, 1.06)	.02	1.05 (1.02, 1.07)	.001
Sex (men vs women)	3.80 (0.42, 34.2)	.23	1.65 (0.68, 4.01)	.27			1.31 (0.64, 2.65)	.46		
MELD (per point)	NA	NA	1.06 (0.99, 1.14)	.09			1.16 (1.11, 1.21)	<.001	1.11 (1.06, 1.17)	<.001
Platelet count per G × L^{-1}	1.00 (1.00, 1.01)	.27	1.00 (0.99, 1.00)	.40			1.00 (1.00, 1.004)	.81		
Albumin per g × L^{-1}	0.76 (0.64, (0.91)	.003	0.90 (0.84, 0.95)	.001	0.88 (0.81, 0.96)	.003	0.94 (0.91, 0.97)	<.001	0.98 (0.88, 0.97)	.002
Bilirubin (per mg × dL^{-1})	1.18 (0.27, 5.20)	.82	1.19 (1.00, 1.42)	.049	0.39 (0.69, 1.12)	.96	1.11 (1.07, 1.15)	<.001		
INR	1.84 (0.14, 24.9)	.65	1.15 (0.42, 3.15)	.79			2.29 (1.34, 3.92)	.002		
Creatinine (per mg × dL^{-1})	0.03 (0.00, 1.83)	.10	1.62 (0.82, 3.19)	.17			1.80 (1.41, 2.30)	.41		
Sodium (per mmol × L^{-1})	1.01 (0.78, 1.30)	.94	0.92 (0.83, 1.03)	.15			0.94 (0.01, 0.98)	.01		
ALP (per U × L^{-1})	1.00 (1.00, 1.01)	.28	1.00 (1.00, 1.01)	.49			1.00 (1.00, 1.007)	.009	1.00 (1.00, 1.01)	.55
GGT (per U × L^{-1})	1.00 (1.00, 1.00)	.03	1.00 (1.00, 1.002)	.45			1.00 (1.00, 1.002)	.77		
AST (per U × L^{-1})	1.00 (0.98, 1.03)	.91	1.00 (0.99, 1.01)	.95			1.01 (1.00, 1.007)	<.001	1.00 (1.00, 1.00)	.07
ALT (per U × L^{-1})	1.00 (0.99, 1.02)	.86	0.99 (0.98, (1.00)	.11			1.00 (1.00, 1.004)	<.001	1.01 (1.00, 1.01)	.57

Note.—Data in parentheses are 95% confidence intervals. ALP = alkaline phosphatase, ALT = alanine transaminase, AST = aspartate transaminase, CACLD = compensated advanced CLD, CLD = chronic liver disease, DACLD = decompensated advanced CLD, FLIS = functional liver imaging score, GGT = γ-glutamyltransferase, INR = international normalized ratio, MELD = model for end-stage liver disease, NA = not applicable, RLE = relative liver enhancement.

predictor of liver-related events (eg, first hepatic decompensation) and transplant-free survival in patients with different causes of chronic liver disease (CLD). Both decompensated and compensated patients with CLD with a reduced FLIS showed a three- to seven-fold higher risk of mortality, even after adjusting for established prognostic factors.

Furthermore, the FLIS proved to be an independent risk factor for a first hepatic decompensation in patients with CACLD. Hepatic decompensation is a key event in the natural history of CLD because patients with CACLD or compensated cirrhosis have a 5-year mortality risk of only 1.5%−10.0% (24,25). However, with the first occurrence of hepatic decompensation (ie, transition to DACLD), the 5-year risk increases to 20%−30%. Accordingly, the main therapeutic goal in CACLD is the prevention of hepatic decompensation by therapeutic interventions (16,26–29). Thus, our results indicated that FLIS as an imaging marker was able to identify patients with CACLD who were at high risk for a first decompensation, potentially warranting more intense treatment strategies.

Conversely, the FLIS was not independently associated with increased risk for the development of further recurrent decompensation in patients with DACLD. The less consistent findings regarding hepatic decompensation are supported by a previous study (30) that investigated the effect of portal hypertension, the main driver of hepatic decompensation, on gadoxetic acid–enhanced MRI. In that study, Asenbaum et al found that neither

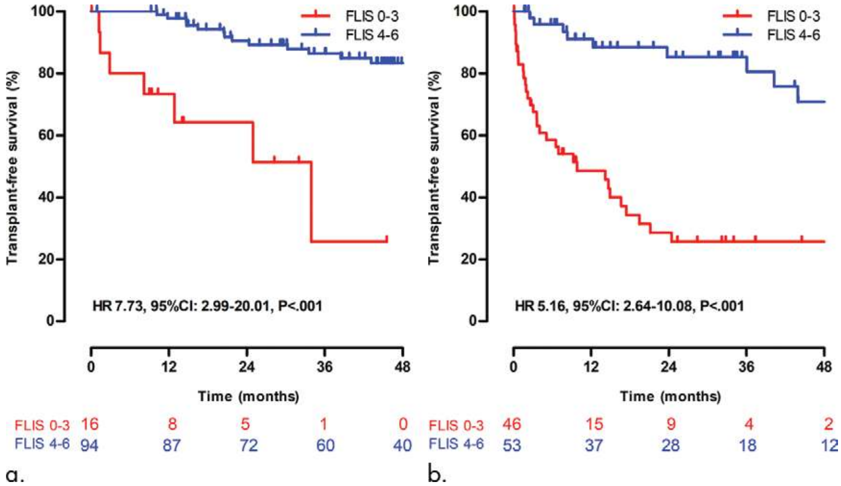

Figure 4: Kaplan-Meier curves for transplant-free survival. Transplant-free survival in patients with **(a)** compensated advanced chronic liver disease, and **(b)** decompensated advanced chronic liver disease. CI = confidence interval, FLIS = functional liver imaging score, HR = hazard ratio.

the parenchymal enhancement, the biliary contrast excretion, nor the portal vein sign were independently associated with the presence of clinically significant portal hypertension (30). Moreover, the lack of an association between FLIS and further hepatic decompensations in patients with DACLD may be because of severe pathophysiologic alterations (eg, bacterial translocation or systemic inflammation) that are only partially related to hepatic function, and thus, are not reflected by the FLIS (31,32), but still trigger further hepatic decompensation.

Our findings are largely in line with those of Yoon et al (33), who found that quantitative assessment of gadoxetic acid uptake was associated with the development of hepatic decompensation in patients with compensated cirrhosis. Similarly, Sandrasegaran et al (34) showed that the relative liver enhancement, which represents liver parenchymal enhancement, is a predictor for the development of hepatic decompensation and mortality in patients with cirrhosis.

Unlike the studies by Asenbaum et al (30) and Yoon et al (33), our cohort included patients at different CLD stages and we separately analyzed patients on the basis of the presence or absence of hepatic decompensation and used a sophisticated multievent analysis that considered the possibility of more than one episode of further hepatic decompensation in the same patient. In addition, we adjusted our MRI metrics for the Model for End-Stage Liver Disease, which may explain the absence of an association with further decompensation in patients with DACLD.

We found excellent inter- and intrareader agreement (intraclass correlation coefficient, >0.89) that underlines the reproducibility and robustness of the FLIS. Furthermore, as a visual tool, followed by simple arithmetic (ie, semiquantitative score), the results are standardized across scanner vendors and field strengths, rendering interoperator variability negligible. It can be used by any radiologist on any MRI system.

Our study had limitations, including its retrospective design, with a possible selection bias. However, because gadoxetic acid–enhanced MRI of the liver is the standard of care for patients with focal liver nodules or masses or CLD at our institution, a selection bias was less likely. Another potential drawback was the lack of histologic proof of the etiologic cause of CLD in most patients; nevertheless, this reflected the reality of the clinical routine.

In conclusion, the functional liver imaging score is a simple noninvasive imaging marker for a first hepatic decompensation and transplant-free survival in patients with advanced chronic liver disease and therefore may provide clinicians with additional prognostic information with which to guide individualized treatment.

Acknowledgment: We acknowledge the great support from the Department of IT-Systems & Communications of the Medical University of Vienna who provided clinical and laboratory data.

Author contributions: Guarantors of integrity of entire study, N.B., L.B., A.B.; study concepts/study design or data acquisition or data analysis/interpretation, all authors; manuscript drafting or manuscript revision for important intellectual content, all authors; approval of final version of submitted manuscript, all authors; agrees to ensure any questions related to the work are appropriately resolved, all authors; literature research, N.B., L.B., S.P.L., D.T., Y.B., M.C.E., H.E., B.S., T.R., A.B.; clinical studies, N.B., L.B., M.M., S.P.L., D.T., Y.B., M.C.E., H.E., G.S., B.S., T.R., A.B.; experimental studies, Y.B., H.E.; statistical analysis, L.B., M.M., S.P.L., D.T., Y.B., H.E., B.S., M.W., A.B.; and manuscript editing, N.B., L.B., M.M., S.P.L., D.T., Y.B., H.E., G.S., B.S., J.C.H., C.S., T.R., A.B.

Disclosures of Conflicts of Interest: **N.B.** disclosed no relevant relationships. **L.B.** disclosed no relevant relationships. **M.M.** disclosed no relevant relationships. **S.P.L.** Activities related to the present article: disclosed no relevant relationships. Activities not related to the present article: disclosed money paid to author for lectures including service on speakers bureaus from Bayer. Other relationships: disclosed no relevant relationships. **D.T.** Activities related to the present article: disclosed no relevant relationships. Activities not related to the present article: disclosed a travel grant from Siemens. Other relationships: disclosed no relevant relationships. **Y.B.** disclosed no relevant relationships. **M.C.E.** disclosed no relevant relationships. **H.E.** disclosed no relevant relationships. **G.S.** disclosed no relevant relationships. **B.S.** Activities related to the present article: disclosed no relevant relationships. Activities not related to the present article: disclosed travel support from AbbVie and Gilead. Other relationships: disclosed no relevant relationships. **M.W.** disclosed no relevant relationships. **J.C.H.** disclosed no relevant relationships. **F.V.** disclosed no relevant relationships. **C.S.** Activities related to the present article: disclosed no relevant relationships. Activities not related to the present article: disclosed board membership from AMRA, Guerbert, Bristol Myers Squibb; consultancies from GE Healthcare, Bayer, ANMRA, Fulcrum Therapeutics, IBM/Watson Health; grants/grants pending from Gilead, GE Healthcare, Siemens, GE MRI, Bayer, GE Digital, GE US, ACR Innovation, Philips, Celgene; royalties from Wolters Kluwer Health for UpToDate; development of education presentations for Medscape, Resoundant. Other relationships: Enanta, ICON Medical Imaging, Gilead, Shire, Virtualscopics, Intercept, Synageva, Takeda, Genzyme, Janssen, NuSirt, Celgene-Parexel, Organovo, Medscape, Epigenomics, Blade, and Boehringer Ingelheim. **T.R.** Activities related to the present article: disclosed no relevant relationships. Activities not related to the present article: disclosed money paid to author for consultancies from AbbVie, Bayer, Boehringer-Ingelheim, Gilead, Intercept, MSD, Siemens; money paid to author for grants/grants pending from AbbVie, Boehringer-Ingelheim, Gilead, MSD, Philips Healthcare, Gore; money paid to author for lectures including service on speakers bureaus from AbbVie, Gilead, Gore, Intercept, Roche, MSD; money paid for travel/accommodations/meeting expenses from Boehringer-Ingelheim, Gilead, and Roche. Other relationships: disclosed no relevant relationships. **A.B.** Activities related to the present article: disclosed no relevant relationships. Activities not related to the present article: disclosed money paid to author for consultancy from Bayer; money paid to author for lectures including service on speakers bureaus from Bayer; money to author's institution for development of educational presentations from Bayer; money paid to author for travel/accommodations/meeting expenses from Bayer. Other relationships: disclosed no relevant relationships.

References

1. Ba-Ssalamah A, Baroud S, Bastati N, Qayyum A. MR imaging of benign focal liver lesions. Magn Reson Imaging Clin N Am 2010;18(3):403–419, ix.
2. Choi SH, Lee SS, Park SH, et al. LI-RADS Classification and Prognosis of Primary Liver Cancers at Gadoxetic Acid-enhanced MRI. Radiology 2019;290(2):388–397.
3. Ba-Ssalamah A, Qayyum A, Bastati N, Fakhrai N, Herold CJ, Caseiro Alves F. P4 radiology of hepatobiliary diseases with gadoxetic acid-enhanced MRI as a biomarker. Expert Rev Gastroenterol Hepatol 2014;8(2):147–160.
4. Yoon JH, Lee JM, Kang HJ, et al. Quantitative Assessment of Liver Function by Using Gadoxetic Acid-enhanced MRI: Hepatocyte Uptake Ratio. Radiology 2019;290(1):125–133.
5. Bastati N, Feier D, Wibmer A, et al. Noninvasive differentiation of simple steatosis and steatohepatitis by using gadoxetic acid-enhanced MR imaging in patients with nonalcoholic fatty liver disease: a proof-of-concept study. Radiology 2014;271(3):739–747.
6. Haider L, Mandorfer M, Güngören Z, et al. Noninvasive Monitoring of Liver Disease Regression after Hepatitis C Eradication Using Gadoxetic Acid-Enhanced MRI. Contrast Media Mol Imaging 2018;2018:8489709.
7. Wibmer A, Prusa AM, Nolz R, Gruenberger T, Schindl M, Ba-Ssalamah A. Liver failure after major liver resection: risk assessment by using preoperative Gadoxetic acid-enhanced 3-T MR imaging. Radiology 2013;269(3):777–786.
8. Theilig D, Steffen I, Malinowski M, et al. Predicting liver failure after extended right hepatectomy following right portal vein embolization with gadoxetic acid-enhanced MRI. Eur Radiol 2019 Mar 21 [Epub ahead of print].
9. Asenbaum U, Kaczirek K, Ba-Ssalamah A, et al. Post-hepatectomy liver failure after major hepatic surgery: not only size matters. Eur Radiol 2018;28(11):4748–4756.
10. Verloh N, Haimerl M, Zeman F, et al. Assessing liver function by liver enhancement during the hepatobiliary phase with Gd-EOB-DTPA-enhanced MRI at 3 Tesla. Eur Radiol 2014;24(5):1013–1019.
11. Utsunomiya T, Shimada M, Hanaoka J, et al. Possible utility of MRI using Gd-EOB-DTPA for estimating liver functional reserve. J Gastroenterol 2012;47(4):470–476.
12. Ba-Ssalamah A, Bastati N, Wibmer A, et al. Hepatic gadoxetic acid uptake as a measure of diffuse liver disease: Where are we? J Magn Reson Imaging 2017;45(3):646–659.
13. Bastati N, Wibmer A, Tamandl D, et al. Assessment of Orthotopic Liver Transplant Graft Survival on Gadoxetic Acid-Enhanced Magnetic Resonance Imaging Using Qualitative and Quantitative Parameters. Invest Radiol 2016;51(11):728–734.
14. Beer L, Mandorfer M, Bastati N, et al. Inter- and intra-reader agreement for gadoxetic acid-enhanced MRI parameter readings in patients with chronic liver diseases. Eur Radiol 2019 Apr 18 [Epub ahead of print].
15. Sterling RK, Lissen E, Clumeck N, et al. Development of a simple noninvasive index to predict significant fibrosis in patients with HIV/HCV coinfection. Hepatology 2006;43(6):1317–1325.
16. de Franchis R; Baveno VI Faculty. Expanding consensus in portal hypertension: Report of the Baveno VI Consensus Workshop: Stratifying risk and individualizing care for portal hypertension. J Hepatol 2015;63(3):743–752https://doi.org/10.1016/j.jhep.2015.05.022.
17. Ripoll C, Groszmann R, Garcia-Tsao G, et al. Hepatic venous pressure gradient predicts clinical decompensation in patients with compensated cirrhosis. Gastroenterology 2007;133(2):481–488.
18. Berzigotti A, Garcia-Tsao G, Bosch J, et al. Obesity is an independent risk factor for clinical decompensation in patients with cirrhosis. Hepatology 2011;54(2):555–561.
19. Scheiner B, Steininger L, Semmler G, et al. Controlled attenuation parameter does not predict hepatic decompensation in patients with advanced chronic liver disease. Liver Int 2019;39(1):127–135.
20. Mandorfer M, Kozbial K, Schwabl P, et al. Changes in HVPG predict hepatic decompensation in patients who achieved SVR to IFN-free therapy. Hepatology 2019 Jul 31 [Epub ahead of print].
21. Therneau TM, Grambsch PM. Modeling survival data: extending the Cox model. New York, NY: Springer Science & Business Media, 2013.
22. Therneau T. A Package for Survival Analysis in S. version 2.38. 2015. https://CRAN.R-project.org/package=survival. Accessed October 28, 2019.
23. Goksuluk D, Korkmaz S, Zararsiz G, Karaagaoglu AE. easyROC: an interactive web-tool for ROC curve analysis using R language environment. R J 2016;8(2):213–230.
24. D'Amico G, Pasta L, Morabito A, et al. Competing risks and prognostic stages of cirrhosis: a 25-year inception cohort study of 494 patients. Aliment Pharmacol Ther 2014;39(10):1180–1193.
25. D'Amico G, Morabito A, D'Amico M, et al. Clinical states of cirrhosis and competing risks. J Hepatol 2018;68(3):563–576.
26. Reiberger T, Ulbrich G, Ferlitsch A, et al. Carvedilol for primary prophylaxis of variceal bleeding in cirrhotic patients with haemodynamic non-response to propranolol. Gut 2013;62(11):1634–1641.
27. Reiberger T, Püspök A, Schoder M, et al. Austrian consensus guidelines on the management and treatment of portal hypertension (Billroth III). Wien Klin Wochenschr 2017;129(Suppl 3):135–158.
28. European Association for the Study of the Liver. EASL Clinical Practice Guidelines for the management of patients with decompensated cirrhosis. [Published correction appears in J Hepatol 2018;69(5):1207.] J Hepatol 2018;69(2):406–460.
29. Ripoll C, Bañares R, Rincón D, et al. Influence of hepatic venous pressure gradient on the prediction of survival of patients with cirrhosis in the MELD Era. Hepatology 2005;42(4):793–801.
30. Asenbaum U, Ba-Ssalamah A, Mandorfer M, et al. Effects of Portal Hypertension on Gadoxetic Acid-Enhanced Liver Magnetic Resonance: Diagnostic and Prognostic Implications. Invest Radiol 2017;52(8):462–469.
31. Bernardi M, Moreau R, Angeli P, Schnabl B, Arroyo V. Mechanisms of decompensation and organ failure in cirrhosis: From peripheral arterial vasodilation to systemic inflammation hypothesis. J Hepatol 2015;63(5):1272–1284.
32. Mandorfer M, Schwabl P, Paternostro R, et al. Von Willebrand factor indicates bacterial translocation, inflammation, and procoagulant imbalance and predicts complications independently of portal hypertension severity. Aliment Pharmacol Ther 2018;47(7):980–988.
33. Yoon JH, Lee JM, Kim E, Okuaki T, Han JK. Quantitative Liver Function Analysis: Volumetric T1 Mapping with Fast Multisection B_1 Inhomogeneity Correction in Hepatocyte-specific Contrast-enhanced Liver MR Imaging. Radiology 2017;282(2):408–417.
34. Sandrasegaran K, Cui E, Elkady R, et al. Can functional parameters from hepatobiliary phase of gadoxetate MRI predict clinical outcomes in patients with cirrhosis? Eur Radiol 2018;28(10):4215–4224.